

Analogue gravity and ultrashort laser pulse filamentation.

D. Faccio^{a,b}, F. Belgiorno^c, S. Cacciatori^{a,d}, M. Clerici^{a,b}, V. Gorini^{a,d}, G. Ortenzi^e, L. Rizzi^a,
E. Rubino^a, V.G. Sala^a.

^a Dipartimento di Fisica e Matematica, Università dell'Insubria, Via Valleggio 11, IT-22100
Como, Italy

^b Consorzio Nazionale Interuniversitario per le Scienze Fisiche della Materia (CNISM), Via
della Vasca Navale 84, Roma, Italy

^c Dipartimento di Matematica, Università di Milano, Via Saldini 50, IT-20133 Milano, Italy

^d Istituto Nazionale di Fisica Nucleare, Piazza dei Caprettari 70, IT-00186, Roma, Italy

^e Dipartimento di Matematica ed Applicazioni, Università degli Studi di Milano Bicocca, Via
Cozzi 53, IT-20125 Milano, Italy

ABSTRACT

Optical pulse propagation in nonlinear Kerr media finds an elegant description in terms of particular space-time metrics. By adopting the language of general relativity and applying standard reasoning developed in the context of quantum fields in curved space-time geometries we may expect to observe effects analogous to Hawking radiation. We discuss recent advances in this field and the application of ultrashort laser pulse filaments for the production of photons by excitation of the electromagnetic quantum vacuum.

Keywords: nonlinear optics, ultrashort laser pulse filamentation, analogue gravity, Hawking radiation

1. INTRODUCTION

The recent surge of interest in the application in optics of geometrical concepts and methods that are usually applied in general relativity, has led to a deeper understanding of light propagation and a number of significant discoveries. One example is the use of metamaterials for invisibility cloaks and perfect lenses.¹ A second example, which we will be treating here, is the description of the quantum properties of moving refractive index media. The space-time geometry of a moving refractive index perturbation (RIP) may lead to the formation of an analogue event horizon, i.e. a trapping region from which light cannot escape, and thus exhibits many features of astrophysical black hole kinematics.²⁻⁴ In 1974 S. Hawking published a paper⁵ entitled “Black-hole explosions?”. The underlying idea is that black-holes, far from being truly black, evaporate, i.e. they emit particles and photons with a blackbody spectrum and with a steadily increasing temperature as their mass decreases, finally leading to an explosion. Although Hawking’s analysis has become a milestone in semiclassical quantum-gravity theory, the question mark in the original paper title still remains due to the lack of any experimental verification of black-hole evaporation. However, such a verification cannot come from direct observation of astrophysical black holes due to the extremely low temperatures of the emitted blackbody spectrum, e.g. of the order of 10 nK for a solar-mass black hole, and will be completely washed out in the surrounding cosmic background radiation at the much higher temperature of 2.7 K. A solution was proposed by Unruh:⁶ gravity and gravitational mass are not actually essential to Hawking radiation. On the contrary, only two fundamental ingredients are required, namely a quantum field, e.g. a fluid or the electromagnetic field and an event horizon induced by a curved space-time metric that traps the quanta of this field, e.g. phonons or photons. Although “gravity” in itself is not strictly required, the study of photon or phonon production from superluminal or supersonic media and the creation of the necessary curved space-time metrics, is usually referred to as “analogue gravity”.

Many proposals have been since put forth, mostly based on analogue Hawking emission in the form of phonons in fluids or Bose-Einstein condensates (BEC) or of photons from moving dielectrics. One of the main difficulties

Further author information: (Send correspondence to D. Faccio)

D. Faccio.: E-mail: daniele.faccio@uninsubria.it, Telephone: +39 031 2386221.

associated to these proposals is, again, the still very low Hawking temperatures predicted by theory. Recently a proposal has been put forth to overcome this difficulty by resorting to an indirect verification of Hawking phonon emission in BECs by measuring an increase in the phonon correlation distribution.⁷ A more direct approach was proposed by Philbin et al. who suggested using an intense optical soliton pulse propagating in a dielectric fiber.³ The soliton intensity is sufficient to induce a refractive index perturbation (RIP) in the fiber medium which in turn acts a space-time curvature of the metric as seen by the quantum electromagnetic vacuum. Due to material dispersion, the RIP will become superluminal, in the sense that it will move faster than the phase velocity of sufficiently blue-shifted wavelengths. These wavelengths will therefore be trapped by the RIP, i.e. an effective trapping event horizon is formed. The important point is that theoretical predictions suggest extremely high Hawking temperatures in the range of thousands of Kelvins and many orders of magnitude higher than in any other physical system proposed to date. We shall show below that crucial features of this model are:

- (i) the intensity of the laser pulse: more intense pulses will induce higher RIP values and possibly a more efficient photon production,
- (ii) the velocity of the laser pulse which can be used, in combination with material dispersion, to tune the spectrum of the emitted Hawking photons,
- (iii) the duration or steepness of the laser pulses which is directly related to the Hawking temperature.

It is therefore essential to control all three of these parameters. Moreover, a delicate issue from an experimental point of view is the ability to identify the electromagnetic radiation associated to the laser pulse which may, due to various nonlinear effects, transform dramatically and cover more than octave in the output spectrum, thus possibly covering any emitted Hawking photons. With these issues in mind, we recently proposed an alternative approach for generating controllable RIPs, namely ultrashort laser pulse filamentation.⁴

Ultrashort laser pulse filamentation may be defined as the spontaneous transformation of an intense laser pulse in a transparent Kerr medium (i.e. with a third order nonlinearity) into a high-intensity spike surrounded by a low-intensity energy reservoir, that propagates apparently without diffraction over distances much longer than the Rayleigh length associated to the spike dimensions.^{8,9} The main features of laser pulse filaments that we will be interested in here are:

- (i) the extremely high peak intensities which may be of the order of tens of TW/cm²,
- (ii) temporal pulse splitting that leads to the formation of two daughter pulses, one traveling faster, the other slower than the input pulse
- (iii) pulse self-compression and the formation of extremely short, even single cycle, pulse structures.

Finally, we also note the possibility to easily separate any Hawking radiation from other nonlinearly generated frequencies as the former may be observed at 90 degrees with respect to the laser pulse propagation axis while the latter are emitted only in the forward direction and within a limited and small cone angle.

2. THEORY

In what follows, we take into consideration the Hawking effect in dielectric black holes. We first show that, under suitable conditions, we can re-map the original Maxwell equations for nonlinear optics into a geometrical description, in analogy to what is done in the case of acoustic perturbations in condensed matter. Then we provide a 2D toy-model in which the presence of the Hawking radiation can be deduced even without recourse to the analogous model characterized by a curved spacetime geometry. This is a very important result from a conceptual point of view, because it represents a corroboration of the analogue picture, using “standard” tools of quantum field theory (i.e. without any reference to the geometric picture). Hawking radiation therefore emerges as a new phenomenon for nonlinear optics, never foreseen before, which could legitimately meet a sceptical attitude by the nonlinear optics community, because of a missing description of the phenomenon by means of the standard tools of quantum electrodynamics. Our aim is to fill this gap and to provide a description of this phenomenon in terms of standard quantum field theory, thus obtaining a double-check which makes the general picture more robust and appealing. A more detailed derivation of the results of this section and a generalization to 4D model may be found elsewhere.¹⁰

2.1 Derivation of the space-time metric.

We start from the generic equation for the electric field in a dielectric medium:

$$\nabla \times \nabla \times \mathbf{E} + \mu_0 \partial_t^2 \mathbf{P} + \frac{1}{c^2} \partial_t^2 \mathbf{E} = 0. \quad (1)$$

Using $\nabla \times \nabla \times \mathbf{E} \simeq -\nabla^2 \mathbf{E}$ we obtain

$$\partial_z^2 \mathbf{E} + \partial_\perp^2 \mathbf{E} - \mu_0 \partial_t^2 \mathbf{P} - \frac{1}{c^2} \partial_t^2 \mathbf{E} = 0. \quad (2)$$

We then write the material polarization as

$$\begin{aligned} \mathbf{P} = & \int_T dt_1 \chi^{(1)}(t-t_1) \mathbf{E}(t_1) + \int_T \int_T dt'_1 dt_2 \chi^{(2)}(t-t_1) \chi^{(2)}(t-t_2) \mathbf{E}(t_1) \mathbf{E}(t_2) \\ & + \int_T \int_T \int_T dt_1 dt_2 dt_3 \chi^{(3)}(t-t_1) \chi^{(3)}(t-t_2) \chi^{(3)}(t-t_3) \mathbf{E}(t_1) \cdot \mathbf{E}(t_2) \mathbf{E}(t_3) + \dots \end{aligned} \quad (3)$$

and we assume that the dielectric is isotropic and therefore $\chi^{(2)}$ is zero. Moreover we assume that the response time T is zero and therefore the χ s do not depend on time. We thus obtain

$$\mathbf{P} = \epsilon_0 \left(\chi^{(1)} \mathbf{E} + \chi^{(3)} |\mathbf{E}|^2 \mathbf{E} + \dots \right) \quad (4)$$

We highlight, in the electric field, two different contributions: $\mathbf{E}_S + \epsilon \mathbf{E}_P$: The first is the contribution related to the pump laser pulse, and the second describes a weak plane wave that “probes” the refractive index perturbation induced by \mathbf{E}_S . For example, the probe wave may even be considered to be a vacuum fluctuation. The small parameter ϵ is the ratio of the amplitudes. Keeping only the first order (in ϵ) contributions we have

$$\partial_z^2 \mathbf{E}_P + \partial_\perp^2 \mathbf{E}_P + \frac{1}{c^2} \left(-\partial_t^2 \mathbf{E}_P - \chi^{(1)} \partial_t^2 \mathbf{E} - \chi^{(3)} \partial_t^2 (|\mathbf{E}_S|^2 \mathbf{E}_P) - 2\chi^{(3)} \partial_t^2 (\mathbf{E}_S \cdot \mathbf{E}_P \mathbf{E}_S) \right) = 0 \quad (5)$$

We then take $|\partial_m u \mathbf{E}_S| \ll |\partial_m u \mathbf{E}_P|$ and find

$$\left(\partial_z^2 + \partial_\perp^2 - \frac{1}{c^2} (1 + \chi^{(1)} + \chi^{(3)} |\mathbf{E}_S|^2) \partial_t^2 \right) \mathbf{E}_P = \frac{2}{c^2} \chi^{(3)} \partial_t^2 (\mathbf{E}_S \cdot \mathbf{E}_P \mathbf{E}_S) \quad (6)$$

We finally take the eikonal approximation for the plane wave which, together with the observation that in our experiments (see below) we only detect photons \mathbf{E}_P that orthogonally polarized with respect to the input pump pulse, \mathbf{E}_S , allows us to put $\partial_t^2 (\mathbf{E}_S \cdot \mathbf{E}_P \mathbf{E}_S) = 0$:

$$\left(\partial_z^2 + \partial_\perp^2 - \frac{1}{c^2} (1 + \chi^{(1)} + \chi^{(3)} |\mathbf{E}_S|^2) \partial_t^2 \right) \mathbf{E}_P = 0 \quad (7)$$

Calling $\mathbf{E}_P = \mathcal{E}_P e^{i\phi}$ we finally obtain

$$k_z^2 + k_\perp^2 - \frac{1}{c^2} (1 + \chi^{(1)} + \chi^{(3)} |\mathbf{E}_S|^2) k_t^2 = 0. \quad (8)$$

The metric is then

$$g_{\mu\nu} = \text{diag}\left(\frac{1}{n^2}, -1, -1, -1\right) \quad (9)$$

where $n^2 = (1 + \chi^{(1)} + \chi^{(3)} |\mathbf{E}_S|^2)$ is the refractive index.

2.2 General Relativity description of the dielectric analogue.

We now consider the model-equation derived above in the 2D limit,

$$\frac{n^2(x-vt)}{c^2} \partial_t^2 \Phi - \partial_x^2 \Phi = 0. \quad (10)$$

$n(x-vt)$ is the refraction index, which has a dependence on spacetime variables which accounts for the propagating refraction index perturbation in the dielectric, which, from an experimental point of view, can be obtained by means of an intense laser pulse in a nonlinear dielectric medium (Kerr effect).

The metric, derived from Eq. (10) is

$$ds^2 = \frac{c^2}{n^2(x-vt)} dt^2 - dx^2. \quad (11)$$

We then pass from the laboratory frame to the pulse frame (refraction index perturbation frame) by means of a boost: $t' = \gamma(t - \frac{v}{c^2}x)$, $x' = \gamma(x - vt)$, so that

$$ds^2 = c^2 \gamma^2 \frac{1}{n^2} \left(1 + \frac{nv}{c}\right) \left(1 - \frac{nv}{c}\right) dt'^2 + 2\gamma^2 \frac{v}{n^2} (1 - n^2) dt' dx' - \gamma^2 \left(1 + \frac{v}{nc}\right) \left(1 - \frac{v}{nc}\right) dx'^2, \quad (12)$$

where $n(x')$ represents a perturbation induced by the laser pulse on top of a uniform background refractive index, n_0 i.e. $n(z, \rho, t) = n_0 + \delta n f(z, t)$, where $f(x, t)$ is a function limited between 0 and 1, that describes the shape of the laser pulse and $\delta n = n_2 I$ where n_2 is the nonlinear Kerr index and I is the laser pulse peak intensity. In general, $\delta n \ll n_0$ in experimental situations.

There is an ergosurface $g_{00} = 0$, i.e. for $1 - n(u) \frac{v}{c} = 0$, which moreover turns out to be lightlike and to correspond to an event horizon, under the conditions

$$\frac{1}{n_0 + \delta n} < \frac{v}{c} < \frac{1}{n_0}, \quad (13)$$

A standard coordinate transformation allows to obtain the metric in a static form: $ds^2 = \frac{c^2}{n^2(x')} g_{\tau\tau}(x') d\tau^2 - \frac{1}{g_{\tau\tau}(x')} dx'^2$, where $g_{\tau\tau}(x') := \gamma^2 \left(1 + n(x') \frac{v}{c}\right) \left(1 - n(x') \frac{v}{c}\right)$. A black hole horizon is easily identified as the greatest solution x'_+ of the equation $g_{\tau\tau}(x') = 0$. The (conformally invariant) temperature is obtained from the surface gravity and is given by¹⁰

$$T' = \gamma^2 v^2 \frac{\hbar}{2\pi k_b c} \left| \frac{dn}{dx}(x'_+) \right|. \quad (14)$$

2.3 Quantum field theory description of the dielectric analogue.

We consider for simplicity a massless scalar field propagating in a dielectric medium and satisfying the equation (10). In order to study our model we adopt the following strategy: a) we develop the WKB approximation in order to write a complete set of solutions of the above equation; b) we pursue a comparison between a initial situation, consisting of an unperturbed dielectric without laser pulse, with a uniform and constant refractive index n_0 , and a final situation where a laser pulse inducing a superluminal pulse is instead present. Our aim is to calculate the mean value of the number of photons (calculated by means of final creation and annihilation operators) on the initial vacuum state. Note that with some abuse of language, we call “photons” the particles associated with our scalar field Φ .

We discuss in the following the solutions of the wave equation both for the final state and for the initial one. We start by considering the out vacuum.

OUT vacuum. In the WKB approximation we put $\Phi = A \exp(ip)$, where the amplitude is considered as slowly varying, and we find the following equation for the phase p :

$$\frac{n(x-vt)}{c} \partial_t p = |\partial_x p|, \quad (15)$$

It is useful to introduce the new variables $u = x - vt$, and $w = x + vt$, in such a way that the equation becomes equivalent to $\left(\frac{n(u)}{c}v \mp 1\right) \partial_w p = \left(\frac{n(u)}{c}v \pm 1\right) \partial_u p$. We find the following form for the general solution:

$$p_+(u, w) = F_+ \left(w - \int^u dy \frac{1 + n(y) \frac{v}{c}}{1 - n(y) \frac{v}{c}} \right) \quad (16)$$

$$p_-(u, w) = F_- \left(w - \int^u dy \frac{1 - n(y) \frac{v}{c}}{1 + n(y) \frac{v}{c}} \right). \quad (17)$$

As for F_{\pm} , we choose $F_{\pm}(y) = \omega y$, i.e. they are chosen to be proportional to the identity function, in analogy to what one expects to find in the case of constant and uniform n . We can point out a very relevant phenomenon. Let us assume that in the integral $\int^u dy \frac{1+n(y)\frac{v}{c}}{1-n(y)\frac{v}{c}}$ the denominator is allowed to vanish, i.e. $1 - n(u)\frac{v}{c} = 0$. In analogy with the general relativity description above, we assume $n = n_0 + \delta n f$ with f a smooth function limited between 0 and 1 (e.g. a normalized gaussian function) we re-obtain the condition (13) obtained in the analogue model.

IN vacuum: For the initial state, we solve the equation

$$\frac{n_0^2}{c^2} \partial_t^2 \Phi - \partial_x^2 \Phi = 0. \quad (18)$$

By choosing the variables $\bar{u} = x - \frac{c}{n_0}t$, $\bar{w} = x + \frac{c}{n_0}t$, we obtain $\partial_{\bar{u}} \partial_{\bar{w}} \Phi = 0$, which is solved trivially by $\exp(-i\omega' \bar{u})$, $\exp(i\omega' \bar{w})$. It is useful to note that the same solution can be easily obtained also in the WKB approximation, through the same choice of independent variables as above.

In order to compare the solutions for the initial situation and the final one, we need to recover a relation between space-time coordinates in the two given situations. One obtains $\bar{u} = \frac{1}{2} \frac{c}{n_0} \frac{k_-}{v} \left(\frac{u}{k} - w \right)$, $\bar{w} = \frac{1}{2} \frac{c}{n_0} \frac{k_-}{v} \left(\frac{w}{k} - u \right)$, where $k_+ = 1 + \frac{v}{c}n_0$, $k_- = 1 - \frac{v}{c}n_0$.

Thermal spectrum.

The Bogoliubov coefficient $\alpha_{\omega\omega'}$ which relates positive frequencies in the initial and final states is given by $\alpha_{\omega\omega'} \sim \frac{1}{2\pi} \sqrt{\frac{\omega'}{\omega}} \tilde{\Phi}_{\omega}(\omega')$, where for $\omega' > 0$:

$$\begin{aligned} \tilde{\Phi}_{\omega}(\omega') &= \int_{-\infty}^{+\infty} du e^{-i\omega' \frac{ck_-}{2vn_0} (k - \frac{1}{k})u} e^{i\omega \frac{2c}{-n'(0)v} \log(u)} \theta(u) \\ &= \int_0^{+\infty} du e^{-i\omega' \frac{2}{k_+} u} e^{i\omega \frac{2c}{-n'(0)v} \log(u)} \end{aligned} \quad (19)$$

Moreover, the Bogoliubov coefficient $\beta_{\omega\omega'}$, which is such that

$$\langle 0 | in | N_{\omega}^{out} | 0 | in \rangle = \sum_{\omega'} |\beta_{\omega\omega'}|^2, \quad (20)$$

satisfies $|\beta_{\omega\omega'}| = |\alpha_{\omega(-\omega')}|$. Then, given the above expression for $\alpha_{\omega\omega'}$, by a suitable choice of the integration contour in the complex plane we find

$$|\alpha_{\omega\omega'}| = \exp\left(\frac{2\pi\omega c}{|n'|v}\right) |\beta_{\omega\omega'}|, \quad (21)$$

which leads to a standard thermal distribution for Bose fields, with temperature¹⁰

$$T = v^2 \frac{\hbar}{2\pi k_B c} \frac{1}{1 - \frac{v}{c}n_0} \left| \frac{dn}{dx}(x_+) \right|. \quad (22)$$

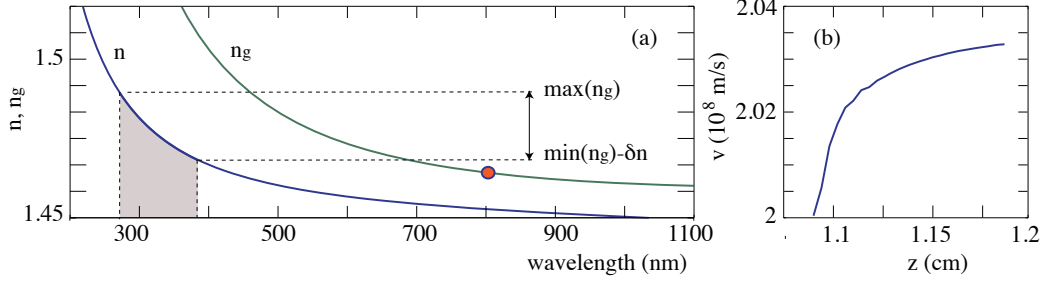


Figure 1. (a) predicted Hawking emission bandwidth based on Eq. (27) and RIP velocity shown in (b), obtained from numerical simulations of filament propagation with the same input conditions used in the experiments.

2.4 Temperature transformation.

The final link between the two models comes from the temperature transformation relation between the co-moving and laboratory reference frames.

We start from Wien's displacement law that gives us the wavelength of maximum emission of a blackbody in function of its temperature:

$$\lambda = \frac{b}{T} \quad \text{with} \quad b = 5.1 \times 10^{-3} \text{ m} \times \text{K}. \quad (23)$$

This gives us an equation for the emitted frequency in the laboratory reference frame

$$\omega = \frac{2\pi c}{b} T. \quad (24)$$

We may transform this frequency to the co-moving reference frame as

$$\omega' = \gamma \frac{2\pi c}{b} T \left(1 - \frac{v}{c} n_0 \right) \quad (25)$$

or, in terms of temperature,

$$T' = \gamma T \left(1 - \frac{v}{c} n_0 \right). \quad (26)$$

This relation links the temperatures in the RIP and laboratory reference frames and is identical to Eq. (14), aside from an additional factor γ which arises from Lorentz contraction of the refractive index derivative dn/dx . This thus underlines the consistency between the analogue Hawking and QED descriptions which indeed lead to blackbody photon distributions with equal temperatures.

2.5 A comment on the event horizon condition.

A crucial point that renders experiments viable is the frequency dependence of n , i.e. material dispersion. In the absence of dispersion a horizon is created only if v is tuned with extreme care such that Eq. (13) is satisfied. Bearing in mind the small values of $\delta n \sim 10^{-3} - 10^{-4}$ (e.g. in fused silica, $n_2 \sim 3 \cdot 10^{-16} \text{ cm}^2/\text{W}$ and $I \sim 10^{13} \text{ W/cm}^2$), this would be no minor feat. Conversely, in the presence of dispersion, $n = n(\omega)$ and Eq. (13) defines a horizon and a spectral emission region for *any* value of v . Figure 1 shows the calculated spectral region for an input laser pulse centered at 800 nm. The material in which the filament and thus the RIP are generated is fused silica. Two curves are shown: the refractive index n and the group index $n_g = n - \lambda dn/d\lambda$ in function of the wavelength λ . Condition (13) may be re-expressed in terms of these indexes as

$$n_g - \delta n < n_H(\omega) < n_g, \quad (27)$$

where n_H indicates the refractive index of the Hawking photons. Note that the Hawking photons will therefore

be emitted only in a bounded spectral window. This is somewhat different from the dispersion-less case in which, once v is properly tuned so as to achieve the horizon condition, all frequencies are excited. This in turn implies that in the dispersion-less case one should expect to observe the complete black-body spectrum predicted by Hawking. Conversely, in the presence of dispersion in our analogue model, only a limited spectral region is excited and the black-body spectral shape will not be discernible. Regarding the width of the spectral emission window we note that this is determined by the value of δn . As a typical case, we consider a gaussian pump pulse in fused silica, $n_g(800 \text{ nm}) = 1.467$ and we find that for $\delta n = 10^{-3}$, Eq. (27) is satisfied over a $\sim 20 \text{ nm}$ bandwidth centered at 435 nm . We note at this point that in real life experiments it is very difficult to keep a perfectly constant v_g . For example if we generate a filament it is known that the v_g , i.e. the n_g varies over the propagation distance. This will lead to a broadening mechanism of the 20 nm bandwidth peak (each value of n_g will generate its own spectral window).

A further issue that then needs to be discussed is the role played by the variation of v_g , i.e. of the RIP acceleration. Figure 1(b) shows the evolution of the trailing filament pulse (indicated with T in Fig. 1(a)) along the propagation direction, calculated using the extended Nonlinear Schrödinger equation with input parameters that describe our experimental settings. We should therefore consider the possibility that the acceleration itself could somehow modify the nature of the emitted photons. For example it is predicted that that an accelerated observer will perceive the background at a higher temperature with respect to an observer in an inertial reference frame. We may qualitatively rule out such effects by noting first of all that the actual variation of the velocity is only of the order of a few percent of the initial pulse velocity and may thus be considered as a small “perturbation” of the ideal, constant velocity case. Moreover, in analogy with a similar reasoning followed by Frolov et al.,¹¹ we note that Hawking photons are expected to be excited from the vacuum in a time, τ , that is the inverse of their frequency (i.e. the photons become real once they are separated by a distance that is at least equal to their wavelength, λ). In the UV region expected for our experiments in fused silica, $\tau \sim \lambda/cn_0 \sim 1 \text{ fs}$. This time is 3 orders of magnitude smaller than the $\sim 1 \text{ ps}$ interval during which the laser pulse accelerates, thus implying that any acceleration-related effects are expected to be negligible on the time scale of Hawking photon production effects.

3. EXPERIMENTS: DIRECT DETECTION OF ANALOGUE HAWKING EMISSION.

3.1 Ultrashort Laser pulse filamentation.

Ultrashort laser pulse filamentation refers to the spontaneous formation of a “filament” of light. The triggering mechanism is the interaction between the intense laser pulse and the medium Kerr nonlinearity which induces a reshaping of the pulse along both the transverse and longitudinal coordinates. In the transverse coordinate, the input pulse will start to shrink under the so-called self-focusing effect and in the longitudinal coordinate self-phase-modulation and dispersion will create new frequencies and distort the pulse. These effects occur concomitantly, leading to the formation of the filament. Notably, the input pulse focuses to a so-called nonlinear focus point at which the highest intensity is reached. This intensity is typically “clamped” to a maximum value that depends mainly on the material properties (e.g. dispersion, nonlinear absorption and ionization) but may vary also with the laser pulse input energy and wavelength. After the nonlinear focus a filament will emerge, i.e. in the transverse coordinate a tightly focused high-intensity spike is observed that propagates apparently without diffraction over long distances. This intensity is surrounded by a much weaker photon bath that co-propagates with the peak and continues to refuel it. The intensity of the central spike will typically start to decay, concomitantly with the formation of two split daughter pulse, one traveling faster and the other slower with respect to the input laser pulse. If the input pulse power is only slightly higher than the filament threshold power, the filament will typically die away. Conversely, significantly higher input powers will lead to a series of refocusing cycles so that a number of successive nonlinear foci will be created, each reaching a similar maximum intensity. If the input power is increased further, then multiple filaments will be observed also in the transverse coordinate, each with its own nonlinear focus and each of which may appear at different propagation distances and, again, with slightly different, yet similar (due to intensity clamping), peak intensities.

The experimental layout is shown in Fig. 2. The input laser pulse is delivered from an amplified Ti:Sapph laser with 35 fs pulse duration, 800 nm central wavelength and $\sim 1 \text{ mJ}$ energy. The pulse is horizontally polarized

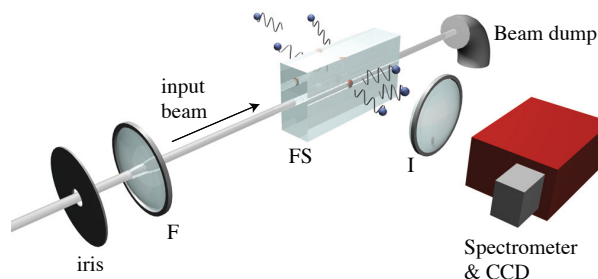


Figure 2. Layout of the experiment. The input beam is focused by the lens F into the Kerr sample (fused silica) and the output beam is collected and removed with a beam dump. Radiation emitted at 90 deg with respect to the beam propagation axis is collected by the lens I, that images the near-field profile of the filament onto the input slit of the imaging spectrometer. The spectrum of this radiation is recorded on a 16 bit, cooled CCD camera.

and loosely focused with a 20 cm focal length lens into a 2 cm long sample of fused silica. The laser pulse undergoes self-focusing and forms a filament. The position of the point of tightest focus (the so-called nonlinear focus) is controlled by an adjustable iris placed before the focusing lens. We observe the filament at 90 deg with respect to the propagation direction. We image the filament onto the input plane of a spectrometer coupled to cooled CCD camera. Therefore, in the configuration adopted in these experiments only photons emitted at 90 deg with respect to the laser pulse propagation direction are collected. This choice solves a number of issues. Indeed, it is necessary to distinguish any signature of Hawking radiation from other spurious effects. Specifically, these are (i) spontaneous Raman emission, (ii) fluorescence from material defects, (iii) Rayleigh scattering and (iv) self-phase-modulation (SPM) induced spectral broadening or four-wave mixing (FWM) due to interaction of the intense laser pulse with the Kerr medium. Rayleigh scattering is absent at 90 deg due to the fact that both the laser pulse and the self-generated supercontinuum signal are horizontally polarized. Moreover, spectral broadening is generated only after the first few mm of propagation after the nonlinear focus (we are imaging less than 1 mm of the initial part of the filament) and in the forward direction within a well-defined cone angle. This radiation was coupled out of the sample and then suppressed with a beam-dump. Four-wave mixing must obey very specific energy and momentum conditions which constrain the emission to well-defined angles. In particular, no emission is allowed at large angles and is zero around 90 deg. Finally, both Rayleigh scattering and nonlinear effects such FWM or SPM have a well-defined polarization, i.e. in an isotropic medium such the one we are using, they are expected to bear the same polarization as the input laser pulse. We directly measured the polarization of the emitted photons (data not shown) by placing a polarizer in front of the spectrometer and we found that they are un-polarized. This therefore excludes the possibility of any contribution from coherent, linear or nonlinear scattering effects arising from the pump laser itself.

Regarding the fluorescences, although fused silica is extremely well characterized and a numerous measurements may be found in literature, we measured their contribution in order to directly evaluate their importance. Figure 3(a) shows an example of the output spectrum at 90 deg over the whole UV to near-infrared range. The different contributions are labelled as: R for the spontaneous Raman emission which reproduces, as expected, the laser pulse spectrum (with a slight Raman-induced red-shift), F1 and F2 for the two observed fluorescences. F1 is due to nonbridging oxygen hole centers (NBOHC) and F2 is due to oxygen deficient centers (ODC).¹² Both of these are first generated by the intense laser pulse and then excited through a 3 photon (with an 800 nm pump laser pulse) or a 4 photon (with a 1055 nm pump laser pulse) absorption process. The F2 fluorescence at 490 nm is particular due to the cumulative nature of the creation process:¹² non-irradiated areas of the sample show a very weak F2 signal, which steadily increases with irradiation and saturates after ~ 1500 laser shots. The presence and excitation of these fluorescences in fused silica is well documented. The shaded area in Fig. 3 highlights the spectral region in which we expect (according to the predictions of our model as described above) to observe Hawking radiation and indeed it appears to be free from fluorescence signals. This was further verified by exciting the medium with a 266 nm laser pulse, obtained as the fourth harmonic from a Nd:glass, 1055 nm central wavelength, 200 fs duration laser pulse. Repeating the predictions above for an input 266 nm wavelength, Hawking radiation is expected to be shifted into the deep-UV region and will therefore not be observable due to absorption and, in any case, due to the limits in the range of the spectrometer and CCD.

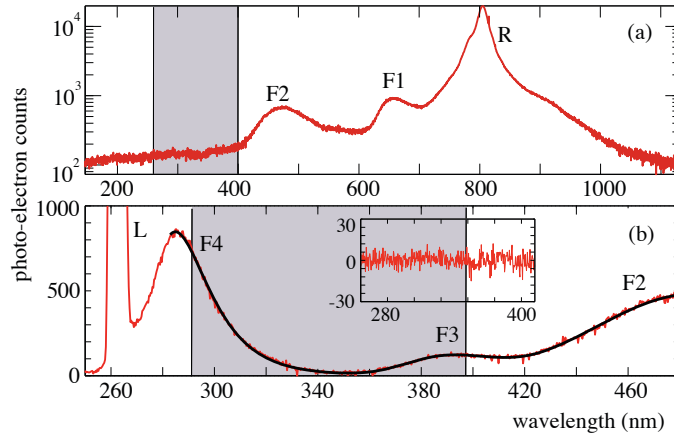


Figure 3. Fluorescence spectra measured at 90 deg with the experimental setup shown in Fig. 2. (a) Spectrum excited by the 800 nm pump pulse: R is the Raman signal, F1 and F2 are the two main fluorescence signals excited through multiphoton processes. (b) Spectrum excited by a 266 nm laser pulse (spectrum indicated with L): F1 and F2 were both visible along with new fluorescence signals, F3 and F4, excited only by 1 photon absorption. The inset shows the photon counts in the 250 nm - 420 nm range after the main fluorescence signals are subtracted out.

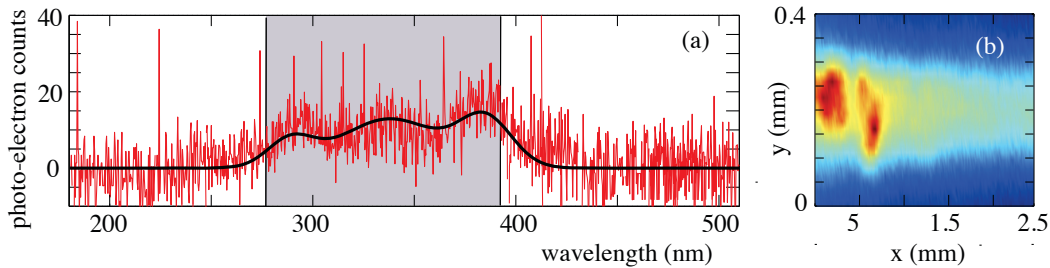


Figure 4. (a) Spectrum of radiation emitted at 90 deg from the filament after subtraction of the fluorescence signal. The spectrum is integrated over 4800 laser shots. The gray shaded area indicated the spectral region predicted in Fig. 1. (b) Near field image of the filament region showing three distinct nonlinear foci.

Conversely, fluorescence signals are known to be optimally excited with 266 nm radiation through 1-photon absorption. Our measurements at 266 nm confirm the fluorescence signals F1 and F2 and, as can be seen in Fig. 4(b) two new weak fluorescence signals, F3 and F4, not excited by the infrared laser pulse, also appear while the shaded area continues to remain substantially free. The black curve represents the best fit obtained (in the frequency domain) with Gaussian functions and once this is subtracted out from the measurement, a featureless signal (shown in the inset) is obtained with an average photo-electron count of 0.7 ± 7 . This therefore proves that there are no fluorescence signals, either known in literature or detectable using our setup, that exhibit the same predicted features of the emitted radiation under examination.

Figure 4 shows the measurements of the spectra around 350 nm excited by the 800 nm laser pulse, integrated over 4800 laser shots, respectively. The measurements shown were performed in sample areas that had not been previously irradiated so as to minimize the contribution from fluorescence signals centered at 490 nm.¹² The red line shows the raw data while the smooth black line serves only as a guide for the eye. There is a clear signal whose position and bandwidth correspond very well to that predicted by our model for analogue Hawking emission. We recall once more that possible contributions from other spurious effects were carefully excluded. If we account for losses and the overall photon collection efficiency of our system we may estimate the total number of photons generated by each laser pulse (over the whole solid angle) to be of the order of 400/pulse. Finally, we note that the Hawking radiation spectrum appears to have a multi-peaked structure. We noted a direct correlation between the number of filaments or nonlinear foci shown in Figs. 3(b), and the number of spectral peaks. The origin of the spectral peaks therefore appears to be due to intensity oscillations related to the formation of multiple filaments and refocusing effects.

4. CONCLUSIONS.

In conclusion we have presented a detailed analysis of a 2D model in which we compare the predictions of the Hawking model for excitation of the quantum vacuum in the presence of an event horizon with the predictions of the QED model for excitation of the quantum vacuum in the presence of a propagating refractive index perturbation. Both models are shown to agree at the quantitative level and predict the emission of photons in well defined spectral regions that depend on the material dispersion and exciting laser pulse velocity. In particular, if the RIP is excited by an intense filament pulse in fused silica, we predict emission in the near-UV region. After carefully excluding spurious effects such as fluorescence, we show measurements of photon emission that agree quantitatively with our predictions. We therefore propose that the emission mechanism of these photons is indeed related to a novel vacuum excitation effect that may also be re-interpreted as evidence of analogue Hawking radiation. Measurements are underway to further corroborate this claim. Generally speaking, these measurements and the underlying theory represent an important step forward in our understanding of the quantum vacuum and of its interaction with intense laser pulses.

ACKNOWLEDGMENTS

The authors acknowledge financial support from the Consorzio Nazionale Interuniversitario per le Scienze Fisiche della Materia (CNISM). Support from P. Di Trapani and help from A. Couairon through the VINO numerical lab is also gratefully acknowledged.

REFERENCES

- [1] U. Leonhardt and T. Philbin, “Transformation optics and the geometry of light,” *arXiv:0805.4778v2*, 2008.
- [2] R. Schützhold, G. Plunien, and G. Soff, “Dielectric black hole analogs,” *Phys. Rev. Lett.* **88**, p. 061101, 2002.
- [3] T. Philbin, C. Kuklewicz, S. Robertson, S. Hill, F. König, and U. Leonhardt, “Fiber-optical analog of the event horizon,” *Science* **319**, p. 1367, 2008.
- [4] D. Faccio, S. Cacciatori, V. Gorini, V. Sala, A. Averchi, A. Lotti, M. Kolesik, and J. Moloney, “Analogue gravity and ultrashort laser pulse filamentation,” *EuroPhys. Lett.* **89**, p. 34004, 2010.
- [5] S. Hawking, “Black hole explosions?,” *Nature* **248**, pp. 30–31, 1974.
- [6] W. Unruh, “Experimental black-hole evaporation?,” *Phys. Rev. Lett.* **46**, p. 1351, 1981.
- [7] R. Balbinot, A. Fabbri, S. Fagnocchi, A. Recati, and I. Carusotto, “Nonlocal density correlations as a signature of hawking radiation from acoustic black holes,” *Phys. Rev. A* **78**, p. 021603, 2008.
- [8] A. Couairon and A. Mysyrowicz, “Femtosecond filamentation in transparent media,” *Phys. Reports* **441**, p. 47, 2007.
- [9] L. Berge, S. Skupin, R. Nuter, J. Kasparian, and J. Wolf, “Ultrashort filaments of light in weakly ionized, optically transparent media,” *Rep. Progr. Phys.* **70**, p. 1633, 2007.
- [10] F. Belgiorno, S. Cacciatori, G. Ortenzi, L. Rizzi, V. Gorini, and D. Faccio, “Dielectric black holes induced by a refractive index perturbation and the hawking effect,” *submitted*, 2010.
- [11] V. Ginzburg and V. Frolov, “Vacuum in a homogeneous gravitational field and excitation of a uniformly accelerated detector,” *Sov. Phys. Usp.* **30**, p. 1073, 1987.
- [12] A. Zoubir, C. Rivero, K. Richardson, M. Richardson, T. Cardinal, and M. Couzi, “Laser-induced defects in fused silica by femtosecond ir irradiation,” *Phys. Rev. B* **73**, p. 224117, 2006.